

# Global transcriptome response to ionic liquid by a tropical rain forest soil bacterium, *Enterobacter lignolyticus*

Jane I. Khudyakov<sup>a,b</sup>, Patrik D'haeseleer<sup>a,c</sup>, Sharon E. Borglin<sup>d</sup>, Kristen M. DeAngelis<sup>a,d</sup>, Hannah Woo<sup>a,d</sup>, Erika A. Lindquist<sup>e</sup>, Terry C. Hazen<sup>a,d</sup>, Blake A. Simmons<sup>a,f</sup>, and Michael P. Thelen<sup>a,b,1</sup>

<sup>a</sup>Deconstruction Division, Joint BioEnergy Institute, Emeryville, CA 94608; <sup>b</sup>Physical and Life Sciences and <sup>c</sup>Computations Directorates, Lawrence Livermore National Laboratory, Livermore, CA 94550; <sup>d</sup>Earth Sciences Division, Ecology Department, Lawrence Berkeley National Laboratory, Berkeley, CA 94720; <sup>e</sup>US Department of Energy Joint Genome Institute, Walnut Creek, CA 94598; and <sup>f</sup>Biomass Science and Conversion Technology Department, Sandia National Laboratories, Livermore, CA 94551

Edited by Steven E. Lindow, University of California, Berkeley, CA, and approved April 9, 2012 (received for review August 6, 2011)

**To process plant-based renewable biofuels, pretreatment of plant feedstock with ionic liquids has significant advantages over current methods for deconstruction of lignocellulosic feedstocks. However, ionic liquids are often toxic to the microorganisms used subsequently for biomass saccharification and fermentation. We previously isolated *Enterobacter lignolyticus* strain SCF1, a lignocellulosic bacterium from tropical rain forest soil, and report here that it can grow in the presence of 0.5 M 1-ethyl-3-methylimidazolium chloride, a commonly used ionic liquid. We investigated molecular mechanisms of SCF1 ionic liquid tolerance using a combination of phenotypic growth assays, phospholipid fatty acid analysis, and RNA sequencing technologies. Potential modes of resistance to 1-ethyl-3-methylimidazolium chloride include an increase in cyclopropane fatty acids in the cell membrane, scavenging of compatible solutes, up-regulation of osmoprotectant transporters and drug efflux pumps, and down-regulation of membrane porins. These findings represent an important first step in understanding mechanisms of ionic liquid resistance in bacteria and provide a basis for engineering microbial tolerance.**

osmotic stress | osmolytes | membrane lipids | differential gene expression | whole genome metabolic reconstruction

**S**ustainable production of biofuels from renewable feedstocks is a key strategy for reducing dependence on fossil fuels and carbon emissions (1). Although lignocellulose stored within the cell wall of plants is one of the largest reserves of convertible energy on the planet, extraction of this resource remains a challenge because of the recalcitrance of the plant cell wall to degradation (2, 3). Cellulose and hemicellulose polysaccharides, the sources of fermentable sugars, are semicrystalline in nature and deeply embedded within a complex network of highly stable lignin polymers (4, 5). Pretreatment of feedstock can remove lignin and reduce cellulose crystallinity, which is critical for improving subsequent saccharification of polysaccharides by enzymes derived from lignocellulosic microorganisms (6). Ionic liquid solvents, a diverse class of molten organic salts, have been used effectively for biomass pretreatment because they disrupt inter- and intramolecular hydrogen bonds within plant cell wall components to improve cellulose recovery, leading to significant improvement of subsequent enzymatic hydrolysis kinetics and product yield (7–10). Nevertheless, one of the problems with using this technology in large-scale industrial biomass pretreatment is its toxicity to microorganisms used in downstream fermentation (11–13).

Although the current standard for a lignocellulosic biofuels process involves discrete production steps, there is a potential economic incentive for unifying the process by using a single engineered strain or collection of strains that would perform both saccharification and fermentation of pretreated biomass during consolidated bioprocessing (CBP) (14–17). The main challenge to this “one pot” strategy is process inhibition of laboratory micro-

organisms by secondary products of polysaccharide catabolism and fermentation, as well as by residual ionic liquid from the pretreatment step (18). For instance, many ionic liquids are highly toxic to microorganisms as a result of the increase in osmotic pressure, potential effects on membrane fluidity and structure, and inhibition of enzymatic activity (11, 13, 19–22); however, the specific mechanisms of toxicity are currently not well-understood, making this an area of intense interest in the field. Because ionic liquids present a promising alternative feedstock pretreatment method, discovery of novel bacterial strains and/or engineering existing strains for ionic liquid tolerance is critical to successful employment of CBP. Utilization of microorganisms isolated from natural environments, such as tropical rain forest (23) soil, can greatly improve the current biofuels strategy. Natural microbial communities that degrade biomass are often exposed to fluctuating environmental conditions, and thus represent a vast resource for both stress-tolerant organisms and highly efficient, stable lignocellulosic enzymes (23–25).

We recently isolated the bacterium *Enterobacter lignolyticus* strain SCF1 from tropical rain forest soil, where microbial communities possess a high potential for both biomass degradation and osmotolerance (23, 26). We report that SCF1 tolerates growth in the presence of >0.5 M 1-ethyl-3-methylimidazolium chloride ([C<sub>2</sub>mim]Cl), an effective biomass pretreatment component (27) that is toxic to most bacteria. The cytotoxicity mechanism of many ionic liquids, specifically [C<sub>2</sub>mim]Cl, has not been investigated; likewise, the molecular basis for rare bacterial tolerance to ionic liquids is not understood. To approach these questions, we used a combination of phenotypic assays and deep sequencing of the SCF1 transcriptome and found that resistance to [C<sub>2</sub>mim]Cl likely involves a functional alteration of cell membrane composition, import and synthesis of compatible solutes, increase in efflux pump

Author contributions: J.I.K., K.M.D., T.C.H., B.A.S., and M.P.T. designed research; J.I.K., S.E.B., K.M.D., and H.W. performed research; P.D., S.E.B., K.M.D., H.W., and E.A.L. contributed new reagents/analytic tools; J.I.K., P.D., S.E.B., H.W., E.A.L., and M.P.T. analyzed data; and J.I.K., P.D., and M.P.T. wrote the paper.

The authors declare no conflict of interest.

This article is a PNAS Direct Submission.

Freely available online through the PNAS open access option.

Data deposition: The genome sequence reported in this paper has been deposited in the GenBank database (accession no. CP002272.1). [This organism was previously called *Enterobacter cloacae* SCF1 and has been renamed *Enterobacter lignolyticus* SCF1. The name has not yet been changed in the National Center for Biotechnology Information (NCBI) database.] The data reported in this paper have been deposited in the Sequence Read Archive (SRA) database, <http://www.ncbi.nlm.nih.gov/sra> [accession nos. SRX059720–SRX059739 (raw Illumina RNA deep sequencing data)].

<sup>1</sup>To whom correspondence should be addressed. E-mail: mthelen@llnl.gov.

This article contains supporting information online at [www.pnas.org/lookup/suppl/doi:10.1073/pnas.1112750109/-DCSupplemental](http://www.pnas.org/lookup/suppl/doi:10.1073/pnas.1112750109/-DCSupplemental).



(Fig. 1A). Parameters, such as lag time, maximum growth rate, and final biomass yield, were obtained using a Gompertz curve-fitting model (30, 32) (Fig. S1).  $[C_2mim]Cl$  increased the lag time at all concentrations tested, and the maximum growth rate was decreased at 187.5 mM  $[C_2mim]Cl$  and above (Table 1). Final biomass yield, as measured by the asymptotic amplitude of the response curve, was decreased at concentrations above 437.5 mM  $[C_2mim]Cl$ . The greatly increased lag time (more than a day at 500 mM  $[C_2mim]Cl$ ) and the somewhat biphasic pattern observed at these high concentrations (Fig. 1 and Fig. S1) suggest that an adaptive change is required to enable ionic liquid tolerance. The biphasic growth observed in Fig. 1B, even with no additions, may be attributable to the fact that the medium is nonoptimal for this environmental bacterium. The effect of ionic liquid on SCF1 growth in TSB10 was also examined by  $OD_{600}$  measurements during 10 h of growth in 0–500 mM  $[C_2mim]Cl$  and was found to mirror the phenotypic microarray results closely (Fig. S2). SCF1 outcompetes several commonly used *Escherichia coli* laboratory strains, including BW25113 (33), which is inhibited by  $[C_2mim]Cl$  concentrations above 250 mM and cannot grow at all in concentrations above 312.5 mM, even in rich medium.

Both lignocellulose dissolution activity and toxicity to microorganisms are mediated by the cation species of ionic liquids (11). We examined if this holds true in our system by testing SCF1 growth in NaCl concentrations ranging from 0–625 mM in a similar experimental setup as  $[C_2mim]Cl$  Omnilog experiments. The results demonstrate that SCF1 is a relatively halotolerant organism that can grow in the presence of up to 625 mM NaCl (Fig. S3), with higher growth rates than in equimolar concentrations of  $[C_2mim]Cl$  (Table S1). Mild growth inhibition was observed at 437.5 mM and above. It is likely that the halotolerant properties of SCF1 contribute to its  $[C_2mim]Cl$  tolerance. We presume it is imidazolium cation, rather than the chloride anion of  $[C_2mim]Cl$ , that is responsible for its toxicity at high concentrations.

Many microorganisms isolated from the environment are able to reduce the toxic effects of anthropogenic compounds, including some ionic liquids, by at least partially metabolizing the chemical (11). The potential ability of SCF1 to degrade ionic liquid was investigated by FTIR spectroscopy measurements of SCF1 culture containing  $[C_2mim]Cl$ . The height of the specific peak corresponding to imidazolium did not change between measurements of culture supernatant before, during, or after a period of active growth, indicating that  $[C_2mim]Cl$  was not degraded by SCF1 during this time (Fig. S4). This is consistent with other reports of low biodegradability of imidazolium-based ionic liquids (34).

**Table 1. Effect of  $[C_2mim]Cl$  on *E. lignolyticus* SCF1 growth**

$[C_2mim]Cl$ , mM	Lag time ( $\lambda$ ), h	Rate ( $\mu_m$ ), h <sup>-1</sup>	Amplitude (A)
0	0.51 ± 0.22	0.146 ± 0.009	2.43 ± 0.04
125	2.81 ± 0.24	0.167 ± 0.014	2.73 ± 0.06
187.5	3.09 ± 0.35	0.137 ± 0.013	2.70 ± 0.07
250	2.51 ± 0.42	0.115 ± 0.015	2.77 ± 0.07
312.5	2.60 ± 0.66	0.092 ± 0.019	2.81 ± 0.08
375	5.60 ± 1.20	0.068 ± 0.021	2.61 ± 0.09
437.5	10.81 ± 1.54	0.061 ± 0.021	2.48 ± 0.09
500	24.34 ± 2.90	0.058 ± 0.016	2.08 ± 0.10
562.5	10.05 ± 3.21	0.026 ± 0.006	1.71 ± 0.15
625	N/A	0.017 ± 0.011	0.67 ± 0.05
Negative control	N/A	0.029 ± 0.013	0.61 ± 0.04

The effects of increasing  $[C_2mim]Cl$  concentration on SCF1 culture lag time ( $\lambda$ ), maximum specific growth rate ( $\mu_m$ ), and asymptotic amplitude of the response (A) were calculated from data presented in Fig. 1A by fitting to the modified Gompertz equation given in *Materials and Methods*. Each parameter is shown as the average of all technical and biological replicates ± SE. Negative control refers to measurements for samples containing culture medium without cells. N/A, not applicable.

**Compatible Solutes and  $[C_2mim]Cl$  Tolerance.** A potential role of compatible solutes (35) in SCF1 ionic liquid tolerance was examined by comparing SCF1 growth in defined medium containing 250 mM  $[C_2mim]Cl$ , either alone or with the addition of 2 mM glycine betaine, proline, ectoine, or glutamate. All four were able to relieve most of the growth inhibition at this intermediate concentration of ionic liquid, as measured by the maximum growth rate and final biomass yield, suggesting that SCF1 can use glutamate, glycine betaine, ectoine, and proline as compatible solutes to tolerate ionic liquid stress (Fig. 1B). Addition of glutamate resulted in the largest improvement in final biomass yield, followed, in decreasing order, by glycine betaine, ectoine, and proline (Table 2). Glutamate and glycine betaine improved final biomass yield to levels observed in defined medium without  $[C_2mim]Cl$ . The greatest improvement in SCF1 maximum growth rate in 250 mM  $[C_2mim]Cl$  was mediated by glycine betaine, followed by glutamate, ectoine, and proline.

**Effect of  $[C_2mim]Cl$  on SCF1 PLFA Composition.** To investigate whether cell membrane reorganization (36) is involved in ionic liquid tolerance, we compared the phospholipid fatty acid (PLFA) profile of SCF1 cells during log phase growth in either TSB10 (control), 375 mM  $[C_2mim]Cl$ , or 375 mM NaCl. The palmitic (16:0), palmitoleic (16:1w7c), vaccenic (18:1w7c), and myristic (14:0) fatty acids made up the majority of total phospholipid composition and did not change significantly in these conditions (Fig. 2A and Table S2). Surprisingly, we did not detect large changes in PLFA components that are altered by stress in other organisms (36–38), with the exception of cyclopropane fatty acids (Fig. 2B). The mole fractions of 17cy and 19cy were dramatically increased in response to  $[C_2mim]Cl$  and NaCl (Fig. 2C and D), with a corresponding decrease in parent monoenoic fatty acids (Fig. 2A). In contrast, other stress indices, such as the ratios of saturated/unsaturated (16:0/16:1 and 18:0/18:1) and stearic/palmitic (18:0/16:0) fatty acids did not change significantly, and did not differ between  $[C_2mim]Cl$  and NaCl treatments (Fig. 2B). Therefore, we found that cyclopropane fatty acids are increased during SCF1 growth with exposure to  $[C_2mim]Cl$ , a response that is partially shared with salt stress.

**$[C_2mim]Cl$ -Induced Changes in Gene Expression.** Global gene expression changes during SCF1 growth with  $[C_2mim]Cl$  were analyzed using Illumina RNA deep sequencing (RNA-Seq) technology (39, 40), with the goal of elucidating molecular mechanisms driving tolerance. Transcriptome libraries were generated from SCF1 cells grown in the absence (control) and presence of  $[C_2mim]Cl$  or NaCl. Two concentrations of stressor were used based on their mild (250 mM) and appreciable (375 mM) inhibitory effects on SCF1 growth, and cells cultured in these conditions were collected during early-phase ( $OD_{600} = 0.2$ ) and active-phase ( $OD_{600} = 0.6$ ) periods of growth representing initial and sustained stress responses (Fig. 3). Of 4,556 genes annotated in the SCF1 genome, 4,399 transcripts were detected by RNA-Seq, with a range of 1.6–7.2 million reads per sample. A wide range of expression patterns was observed, but the most significant overall changes in gene expression occurred at  $OD_{600} = 0.6$  in 375 mM  $[C_2mim]Cl$  and NaCl; consequently, detailed analysis was focused on these specific libraries.

Differential expression (DE) analysis of RNA-Seq data using the DESeq software package (41) revealed 1,245 genes with significant differential expression and an increase of twofold or greater in  $[C_2mim]Cl$  vs. NaCl (Fig. 3B). Only 688 genes showed significant differential expression in  $[C_2mim]Cl$  vs. control, partly because the two control replicates at  $OD_{600} = 0.6$  were less well-correlated, such that a higher fold-change was required to reach statistical significance (Fig. 3A). We found that the SCF1 response to  $[C_2mim]Cl$  was significantly different from the  $\sigma^S$ -regulated general stress response in *E. coli*. Weber et al. (42) identified 140  $\sigma^S$ -dependent genes in *E. coli* up-regulated during

**Table 2. Effect of compatible solutes on *E. lignolyticus* SCF1 growth**

Growth condition	Growth rate ( $\mu_m$ ), h <sup>-1</sup>	Amplitude (A)
0 mM [C <sub>2</sub> mim]Cl	0.146 ± 0.009	2.50 ± 0.10*
250 mM [C <sub>2</sub> mim]Cl	0.111 ± 0.011	1.55 ± 0.08
250 mM [C <sub>2</sub> mim]Cl + proline	0.126 ± 0.009	2.38 ± 0.09*
250 mM [C <sub>2</sub> mim]Cl + ectoine	0.128 ± 0.007	2.43 ± 0.10*
250 mM [C <sub>2</sub> mim]Cl + glycine betaine	0.137 ± 0.010	2.53 ± 0.13*
250 mM [C <sub>2</sub> mim]Cl + glutamate	0.130 ± 0.008	2.57 ± 0.11*
Negative control	0.027 ± 0.003	0.46 ± 0.03*

Effects of addition of 2 mM proline, ectoine, glycine betaine, and glutamate on SCF1 growth with 250 mM [C<sub>2</sub>mim]Cl in defined medium. Maximum specific growth rate ( $\mu_m$ ) and asymptotic amplitude of the response (A) were calculated from data presented in Fig. 1B by fitting to the modified Gompertz equation given in *Materials and Methods*. Each parameter is shown as the average of all technical and biological replicates ± SE. Negative control refers to measurements for samples containing culture medium without cells.

\*Denotes amplitude (A) values that differed significantly from those for the 250 mM [C<sub>2</sub>mim]Cl condition by *t* test ( $P < 0.01$ ).

short and long-term stress responses, including osmotic and pH shock, as well as transition into stationary phase. Eighty-one of these nonspecific stress response genes had a bidirectional best BLAST hit at >70% sequence identity to SCF1. However, only 27 of these orthologs were significantly differentially expressed in [C<sub>2</sub>mim]Cl vs. NaCl, accounting for less than 4% of the 688 differentially expressed genes, and included none of the top 50 genes with highest fold-change under those conditions.

We found that transporters accounted for more than a quarter of functional gene categories differentially expressed in [C<sub>2</sub>mim]Cl vs. NaCl (Fig. 4A). Translation; ribosomal structure; and biogenesis genes, including ribosomal gene clusters, were strongly down-regulated, followed by nucleotide metabolism; cell wall/membrane/envelope biogenesis; and replication, recombination, and repair genes. In contrast, energy production and conversion as well as amino acid and carbohydrate metabolism were up-regulated. Results for [C<sub>2</sub>mim]Cl vs. control were broadly similar, with some notable exceptions: [C<sub>2</sub>mim]Cl vs. control demonstrated only half as many up-regulated transporters (65 up-regulated transporters for [C<sub>2</sub>mim]Cl compared with 128 up-regulated transporters for control), whereas [C<sub>2</sub>mim]Cl vs. salt showed far more up-regulated proteins of unknown function and hypothetical proteins for [C<sub>2</sub>mim]Cl than for salt (*SI Materials and Methods*).

The effect of [C<sub>2</sub>mim]Cl stress on SCF1 metabolism was examined by mapping RNA-Seq data onto a reconstruction of SCF1 metabolic pathways using Pathway Tools (43) software (Fig. 5). Pathways that were up-regulated specifically in [C<sub>2</sub>mim]Cl rather than NaCl conditions included those for cyclopropane fatty acid synthesis, fatty acid  $\beta$ -oxidation, lipid biosynthesis, and amino acid degradation and conversion. Consistent with results of PLFA analysis, we found that the cyclopropane fatty acyl phospholipid synthase transcript was up-regulated fivefold in ionic liquid-exposed cells compared with control (Fig. 5a), whereas salt stress caused only a modest 1.3-fold increase. Many of the fatty acid  $\beta$ -oxidation pathways were also up-regulated (Fig. 5b), and a number of other fatty acid and lipid biosynthesis pathways showed shifts from one isozyme to another. One of the most highly down-regulated pathways in [C<sub>2</sub>mim]Cl was the enterobactin biosynthesis pathway encoded by the *entCEBAH* operon (Entcl\_3202–Entcl\_3198), which showed a 66-fold down-regulation compared with either control or NaCl (Fig. 5c). A variety of amino acid degradation and conversion pathways were up-regulated in [C<sub>2</sub>mim]Cl vs. salt, some of which may be involved in production of compatible solutes, such as glutamate or glutamine (Fig. 5d).

Sugar, amino acid, and peptide transporters were up-regulated in [C<sub>2</sub>mim]Cl (Fig. 4B), consistent with up-regulation of the corresponding metabolic pathways and energy metabolism shown in Fig. 5. A wide variety of Fe<sup>2+</sup>, Fe<sup>3+</sup>, heme, and siderophore transporters were strongly down-regulated. There was

a larger number of significantly down-regulated than up-regulated drug efflux pumps; however, some of the up-regulated drug efflux pumps showed very high fold-changes (Table 3). One of the most highly up-regulated transporter operons in both [C<sub>2</sub>mim]Cl and NaCl encodes a glycine betaine/L-proline ATP-binding cassette (ABC) transporter, which was up-regulated 63-fold in [C<sub>2</sub>mim]Cl and 167-fold in NaCl vs. control. Three porins were down-regulated in both [C<sub>2</sub>mim]Cl and NaCl vs. control, two of which had extremely high RNA-Seq expression counts: Entcl\_4131 (porin LamB type), which was down-regulated 19-fold in [C<sub>2</sub>mim]Cl and 10-fold in NaCl, was the 27th most abundant transcript in the entire control library normalized by transcript length, and Entcl\_2856 (porin Gram-negative type), which was down-regulated threefold in [C<sub>2</sub>mim]Cl and NaCl, was the third most abundant transcript in control cells (Table 3).

Technical and biological validation of RNA-Seq data was performed by RT-quantitative PCR (qPCR) using nine genes with distinct changes in expression between conditions, including genes of interest, such as cyclopropane fatty acyl synthase, major facilitator superfamily (MFS) efflux pump, and ABC family glycine betaine/proline transporter (Fig. S5). We found that gene expression changes were highly correlated between RNA-Seq and qPCR data. In addition, changes in expression of these specific transcripts were mirrored in an independently conducted biological experiment, validating that they were consistently affected by [C<sub>2</sub>mim]Cl exposure.

## Discussion

Bacterial strains isolated from such environments as forest soils, which experience fluctuating nutrient, temperature, oxygen, and water levels, have been found to be extremely robust compared with model laboratory organisms, which succumb to process inhibition at almost every step during biofuels production (18). For instance, we found that *E. coli* strain BW25113 growth was completely inhibited by [C<sub>2</sub>mim]Cl concentrations above 312.5 mM. Likewise, other strains of *E. coli* show high sensitivity to a number of ionic liquids (19–21). Because residual ionic liquids in pretreated feedstocks can be highly toxic to many microorganisms, identifying microbes that possess both high degradation activity and stress tolerance and developing an understanding of the underlying mechanisms are critical to engineering effective strains for the biofuels process.

*E. lignolyticus* SCF1 is a facultatively anaerobic, fast-growing, and moderately halotolerant bacterium isolated from tropical rain forest soil that can grow in the presence of 0.5 M [C<sub>2</sub>mim]Cl. Using RNA-Seq, a powerful tool for transcriptomics (39, 40), we analyzed transcriptional changes during SCF1 exposure to [C<sub>2</sub>mim]Cl and found that the molecular avenues affected included compati-



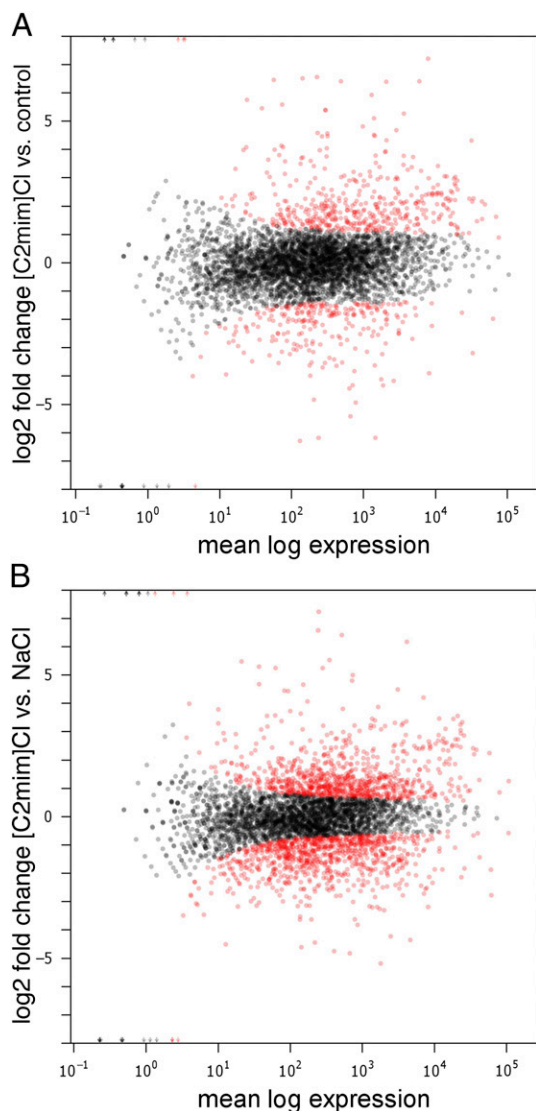


**Fig. 3.** Statistical analysis of differential gene expression. Plots of  $\log_2$  ratio (fold-change) vs. the mean of the log expression levels in the two conditions, for 375 mM  $[C_2mim]Cl$  vs. control (A) and 375 mM  $[C_2mim]Cl$  vs. 375 mM NaCl (B), at  $OD_{600} = 0.6$ . Red dots indicate genes detected as differentially expressed at a 10% false discovery rate. Arrows at the upper and lower plot borders indicate genes with very large or infinite log fold-change.

Other studies will be necessary to determine the extent to which these molecules accumulate intracellularly.

A number of multidrug efflux pumps, such as those of the MFS, were highly up-regulated by  $[C_2mim]Cl$ . Although the single-imidazole ring structure of  $[C_2mim]Cl$  does not resemble antibiotics that are predicted substrates for these transporters, some efflux pumps are promiscuous to some extent, and may therefore pump other toxic compounds out of the cell, such as ionic liquids (46). Efflux pumps contribute greatly to microbial resistance to toxic compounds (47), and their heterologous expression can improve tolerance of *E. coli* to hydrocarbons (48); thus, it is likely that these pumps could play a similar role in  $[C_2mim]Cl$  tolerance.

Another approach to reducing toxicity is to decrease passive membrane permeability to the stressor (e.g., by decreasing expression of membrane porins) (49). We found that two porin genes that were among the most highly expressed transcripts in the control condition were strongly down-regulated in SCF1 cells exposed to  $[C_2mim]Cl$ . Regulation of porin expression has been

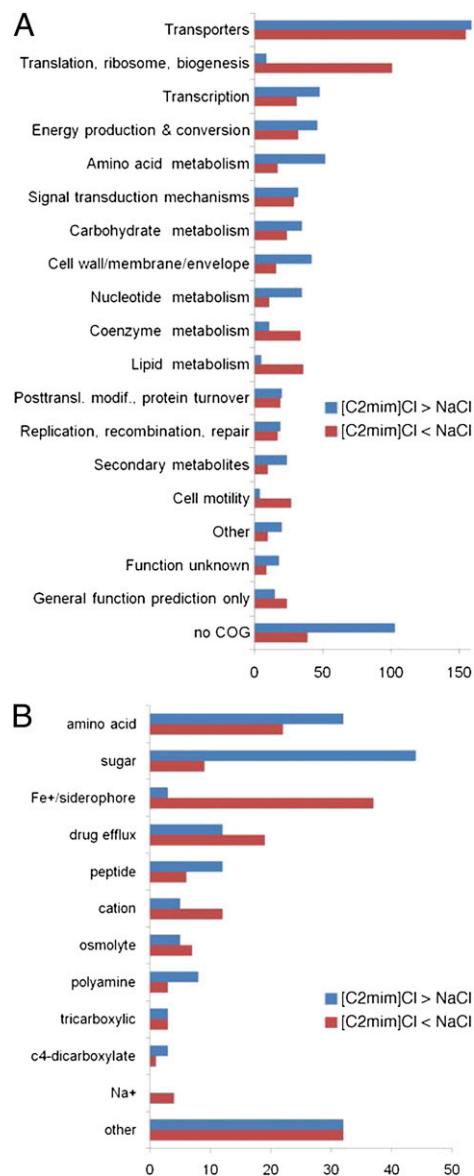


**Fig. 4.** Categories of differentially expressed genes in  $[C_2mim]Cl$  vs. NaCl. Genes differentially expressed in 375 mM  $[C_2mim]Cl$  vs. 375 mM NaCl at  $OD_{600} = 0.6$  were divided into nontransporters (A) and transporters (B). Nontransporters were characterized by clusters of orthologous groups (COG) categories (72, 75). Transporter genes were categorized based on predicted substrate type in TransportDB (45). Blue bars indicate number of genes up-regulated in  $[C_2mim]Cl$  ( $[C_2mim]Cl > NaCl$ ), whereas red bars indicate numbers of genes up-regulated in NaCl ( $[C_2mim]Cl < NaCl$ ).

implicated in antibiotic resistance in a number of bacterial organisms, as well as in acid resistance in Enterobacteriaceae (47, 49). Therefore, the combination of reduced cell permeability and active pumping may limit the intracellular ionic liquid concentration, thus reducing its toxicity to the microorganism.

Cell membrane permeability can also be reduced by modifying the PLFA composition (36). We found that  $[C_2mim]Cl$  exposure caused an increase in cyclopropane fatty acids with a concomitant decrease in the parent monoenoic fatty acids, without significant alteration in other cell membrane components. Using an independent method, we also detected an increase in transcripts of cyclopropane fatty acyl synthase, the enzyme responsible for cyclopropanation, during SCF1 growth with  $[C_2mim]Cl$ . This response was also seen with NaCl stress but to a lesser degree.

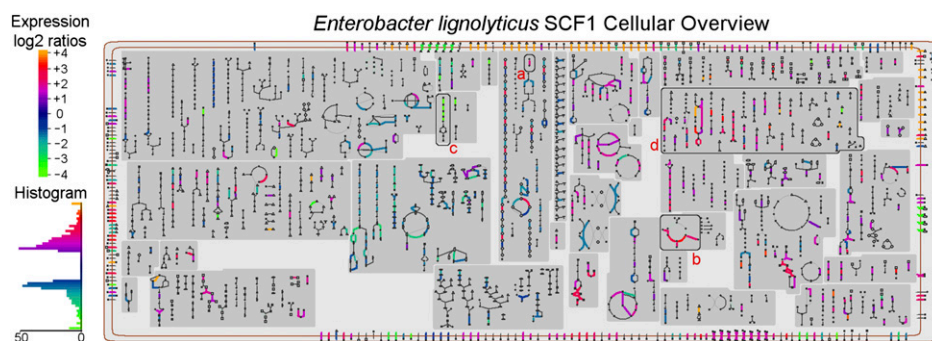


**Fig. 5.** Whole-genome metabolic reconstruction of SCF1 showing differentially expressed pathways and transporters. Metabolic reconstruction was performed using TransportDB (45) as described in *Materials and Methods*. Reactions in the network corresponding to significantly over- or underexpressed genes in 375 mM [C<sub>2</sub>mim]Cl vs. 375 mM NaCl were colored based on their log ratio, ranging from orange for log ratio >4.0 (16-fold or more up-regulated in [C<sub>2</sub>mim]Cl) to light green for log ratio <-4.0 (16-fold or more up-regulated in NaCl). Transporters are arranged around the boundary. Selected enzymatic reactions or pathways include cyclopropane synthesis (a), fatty acid  $\beta$ -oxidation (b), enterobactin biosynthesis (c), and amino acid degradation and conversion (d).

Given the pronounced shift in cyclopropane fatty acids and the widespread differences in other metabolic pathways between [C<sub>2</sub>mim]Cl and salt exposure, it is somewhat unexpected that the changes in PLFA profiles between these conditions are otherwise fairly similar, presumably attributable to a generalized membrane response to osmotic stress. However, the increase in cyclopropane fatty acid production during [C<sub>2</sub>mim]Cl exposure demonstrates the distinct effect of ionic liquid on the bacterium. A number of studies using *E. coli* and lactobacilli have demonstrated that methylation of the *cis*-acyl chain double bond to form a cyclopropane ring plays a significant role in tolerance to acid, salt, butanol, and other stressors by reducing membrane fluidity and decreasing permeability (50–54). It is probable that cyclopropane fatty acid production plays a similar role in [C<sub>2</sub>mim]Cl tolerance by stabilizing the cell membrane. Furthermore, up-regulation of fatty acid  $\beta$ -oxidation pathways and changes in other lipid biosynthesis genes suggest that cell membrane remodeling is an important component of the response to ionic liquids. It remains

to be seen whether [C<sub>2</sub>mim]Cl or other ionic liquids, such as [C<sub>2</sub>mim]acetate (OAc), cause a similar up-regulation in *cfa* and 17cy and 19cy production in *E. coli*, and whether this pathway can be enhanced to improve tolerance of ionic liquids.

The up-regulation of sugar and amino acid metabolism and transporters, combined with down-regulation of ribosomal clusters and nucleotide synthesis, suggested that the organism may be diverting energy from cell replication toward fighting the effects of [C<sub>2</sub>mim]Cl toxicity. The strong down-regulation of a wide variety of iron uptake and scavenging mechanisms, including enterobactin biosynthesis, export, and reuptake, as well as heme, siderophore, ferric, and ferrous iron transporters, indicated an as yet unexplained involvement of iron homeostasis in [C<sub>2</sub>mim]Cl toxicity or tolerance, possibly involving activation of the global *Fur* regulon. The homologous *Fur* regulator in SCF1 (Entcl\_3132) was not differentially expressed in our RNA-Seq data, but *Fur* activity is typically regulated after translation by binding to Fe<sup>2+</sup> (55). It is possible that [C<sub>2</sub>mim]Cl toxicity causes an increase in free in-

**Table 3.** Top SCF1 transporter genes with significant change in expression in [C<sub>2</sub>mim]Cl relative to control and NaCl

Locus tag	Control	[C <sub>2</sub> mim]Cl	NaCl	Log <sub>2</sub> [C <sub>2</sub> mim]Cl/control	Log <sub>2</sub> [C <sub>2</sub> mim]Cl/NaCl	Substrate
Entcl_1711	278	2,646	69	3.25	5.27	Amino acid
Entcl_2390	223	463	16	1.06	4.83	Aromatic amino acid
Entcl_2352	5	400	16	6.33	4.69	Multidrug efflux
Entcl_1686	7	211	9	4.87	4.52	Malonate
Entcl_1685	45	1,428	96	4.97	3.90	Sodium ion/citrate symporter
Entcl_0539	6,677	11,886	1,226	0.83	3.28	Taurine
Entcl_0439	831	1,858	195	1.16	3.25	Amino acid
Entcl_1261	32	247	26	2.94	3.22	Ribose
Entcl_1260	24	136	16	2.51	3.08	Ribose
Entcl_1262	18	105	12	2.55	3.07	Ribose
Entcl_3205	6	0	6	N/A	N/A	Ferric enterobactin
Entcl_3582	147	9	178	-4.07	-4.35	Cobalamin/Fe <sup>3+</sup> -siderophores
Entcl_3204	93	6	126	-3.93	-4.36	Multidrug efflux
Entcl_3206	47	3	71	-4.02	-4.59	Ferric enterobactin
Entcl_3912	1,975	136	2,880	-3.86	-4.41	Trehalose
Entcl_3119	2	5	114	1.28	-4.58	Potassium ion
Entcl_3274	112	45	1,187	-1.30	-4.71	C4-dicarboxylate
Entcl_1546	2,627	45	1,359	-5.87	-4.92	Siderophore
Entcl_3210	55	1	43	-5.52	-5.17	Iron
Entcl_3211	21,041	147	10,013	-7.16	-6.09	Siderophore

Top SCF1 transporters affected by ionic liquid are shown as the 10 most up-regulated (highest log ratios) and 10 most down-regulated (lowest log ratios) genes in 375 mM [C<sub>2</sub>mim]Cl relative to 375 mM NaCl. Normalized gene counts are shown for SCF1 cells cultured in TSB10 alone (control), 375 mM [C<sub>2</sub>mim]Cl, and 375 mM NaCl. Log ratio calculations and predicted transporter substrate assignments were performed as described in *Materials and Methods*. N/A, not applicable (transcripts were not detected in 375 mM [C<sub>2</sub>mim]Cl).

tracellular Fe (e.g., by disrupting formation or increasing degradation of iron-containing proteins or prosthetic groups).

In conclusion, we propose a preliminary ionic tolerance model for bacteria like SCF1, involving (i) rapid phospholipid cell membrane remodeling and down-regulation of porins to decrease cell permeability to ionic liquid; (ii) up-regulation of multidrug efflux pumps to reduce intracellular ionic liquid concentration; and (iii) increase in compatible solute scavenging, transport, and synthesis to reduce adverse osmotic pressure effects of residual ionic liquid influx. This model remains to be tested by direct intracellular measurements of [C<sub>2</sub>mim]Cl concentration during SCF1 exposure to this ionic liquid, although a current limitation of this approach is the difficulty in resolving subcellular localization and temporal dynamics of ionic liquids in single cells. It will also be important to determine whether this model is applicable to other ionic liquids used for biomass pretreatment, such as [C<sub>2</sub>mim]OAc. In the meantime, however, we have found that RNA-Seq is a highly effective, reproducible approach for investigating the global bacterial response to a “novel” chemical at the transcriptome level. The results presented here provide an important basis for further work in tolerant strain engineering and for understanding microbial stress and adaptation responses to anthropogenic chemicals used in industry.

## Materials and Methods

**Strains and Culture Conditions.** *E. lignolyticus* strain SCF1 was isolated from tropical forest soils collected from the Short Cloud Forest site in the El Yunque National Forest in Puerto Rico (26). SCF1 growth assays were performed aerobically at 30 °C in TSB10. The osmolality of TSB10 is ~30 mOsm/kg based on that reported for trypticase soy broth (TSB) (56). MOD-CCMA-defined medium (26) for osmoprotectant experiments contained the following: 2.8 g·L<sup>-1</sup> NaCl, 0.1 g·L<sup>-1</sup> KCl, 27 mM MgCl<sub>2</sub>, 1 mM CaCl<sub>2</sub>, 1.25 mM NH<sub>4</sub>Cl, 9.76 g·L<sup>-1</sup> MES, 1.1 mL·L<sup>-1</sup> K<sub>2</sub>HPO<sub>4</sub>, 12.5 mL·L<sup>-1</sup> trace minerals (57, 58), 1 mL·L<sup>-1</sup> Thauer's vitamins (59), 20 mM D-glucose, and 0.1% yeast extract. The *E. coli* strain used for stress tolerance experiments was BW25113, a derivative of the *E. coli* K-12 strain BD792. BW25113 was used to make the Keio KO collection of single-gene KOs, and it has the genotype  $\Delta(\text{araD-araB})567$ ,  $\Delta(\text{lacZ4787}::\text{rrnB-3})$ ,  $\lambda$ -, *rph-1*,  $\Delta(\text{rhaD-rhaB})568$ , *hsdR514* (33). *E. coli* growth assays were performed at 37 °C in Luria-Bertani-Miller broth. Several media constituents, including TSB, were obtained from EMD Chemicals, Inc. The [C<sub>2</sub>mim]Cl, NaCl, proline, ectoine, glycine betaine, glutamate, and D-glucose were obtained from Sigma-Aldrich.

**Omnilog Phenotypic Microarray Assays.** SCF1 was cultured in 50 mL of TSB10 until OD<sub>600</sub> = 0.4 at 30 °C with shaking at 200 rpm and used to inoculate empty sterile multiwell plates (Biolog, Inc.) at a 10% (vol/vol) dilution of a total volume of 100  $\mu$ L. A range of [C<sub>2</sub>mim]Cl or NaCl concentrations (0–625 mM) in TSB10 was tested in each plate using the empty plate function. After addition of proprietary Redox Dye A (Biolog, Inc.) according to the manufacturer's instructions, multiwell plates were incubated in the Omnilog instrument at 30 °C for 72 h. Three biological replicates were grown in parallel within the same run. Growth in each 100- $\mu$ L well was measured in Omnilog (OL) units, calculated as the change in tetrazolium redox dye color intensity attributable to dye reduction during cell respiration (29). Dye intensity values were measured at 15-min intervals throughout the incubation period. Results are reported as the natural log of average OL values (average of 6 technical replicate wells for each of 3 biological replicate plates, with the exception of the experiment presented in Fig. 1B, for which only 2 biological replicates were used). A negative control containing medium and dye with no cells was run in each plate to rule out contamination and obtain background readings. *E. coli* experiments were performed similarly using Luria-Bertani-Miller broth as the base medium at 37 °C incubation temperature.

**Omnilog Curve Fitting and Growth Parameters.** Omnilog growth curve data were log-transformed and fitted to a modified Gompertz equation (30, 32):

$$\ln(N) = \ln(N_0) + A \exp \left\{ - \exp \left[ \frac{H_m e}{A} (\lambda - t) + 1 \right] \right\},$$

where  $N_0$  is the lower asymptote for the color intensity (fitted as a separate parameter of the growth curve, because the initial color intensity at time 0 is highly sensitive to measurement noise at low intensity levels),  $\lambda$  is the lag

time before onset of exponential growth (constrained to be greater than or equal to 0),  $\mu_m$  is the maximum specific growth rate, and  $A$  is the asymptotic response. These parameters are demonstrated in Fig. S1B. For visualization purposes, the growth curve data in Fig. 1 and Fig. S1 was slightly smoothed using a Gaussian kernel ([1 4 6 4 1]) to reduce some of the measurement noise.

**FTIR Determination of Ionic Liquid Concentration.** [C<sub>2</sub>mim]Cl was measured quantitatively on a VERTEX 70 Series FTIR Spectrometer (Bruker Optics) by recording the unique peak height at 1,170.59 cm<sup>-1</sup> corresponding to imidazolium-based ionic liquid. Supernatants of SCF1 cultures in TSB10 (baseline control) or TSB10 with 272.8 mM [C<sub>2</sub>mim]Cl were collected after 6.9 h and 24.3 h of growth and analyzed by FTIR. A standard curve was prepared using 0 mM, 34.1 mM, 68.2 mM, 136.4 mM, 204.6 mM, and 272.8 mM [C<sub>2</sub>mim]Cl in TSB10. Averaged peak height values for three biological replicates were used to calculate the concentration of ionic liquid remaining in culture from the standard curve equation.

**PLFA.** SCF1 cells cultured in 40 mL of TSB10 (control), 375 mM [C<sub>2</sub>mim]Cl, or 375 mM NaCl were grown until OD<sub>600</sub> = 0.6 and then collected on Sterivex GP 0.22- $\mu$ m filter units (Millipore). Fatty acid methyl esters were extracted by the Bligh-Dyer method (60–62), detected on an Agilent 6890N GC/MS instrument on an HP1 60-m column  $\times$  0.25-mm inner diameter, and quantified by comparison to known standards. Average masses of all lipids profiled for triplicate biological samples are given in Table S2. Stress indicators were calculated as ratios of saturated/unsaturated, cyclopropane/unsaturated, and 18:0/16:0 lipids (60, 63–67).

**Total RNA Isolation.** SCF1 cultures in TSB10 (control), 250 mM [C<sub>2</sub>mim]Cl, 375 mM [C<sub>2</sub>mim]Cl, 250 mM NaCl, and 375 mM NaCl were collected at OD<sub>600</sub> = 0.2 and OD<sub>600</sub> = 0.6, and treated with RNA Protect reagent (Qiagen) according to the manufacturer's protocol. RNA extraction and purification were performed with the RNeasy Miniprep Kit (Qiagen) using 2 mg/mL lysozyme for cell lysis (Sigma-Aldrich) and including on-column DNase digest (Qiagen). Residual genomic DNA contamination was removed by TURBO DNase I (Ambion) treatment according to the manufacturer's protocol. Samples were purified by phenol/chloroform/isoamyl alcohol (25:24:1, pH 8; Sigma-Aldrich) extraction and precipitated with 3 M NaOAc (Fermentas). RNA pellets were resuspended in diethyl pyrocarbonate (DEPC)-treated water (Ambion), and sample concentration was quantified using the Qubit RNA-specific fluorescent dye assay system (Invitrogen). RNA integrity was assayed using the RNA Nano 6000 chip on the Bioanalyzer system (Agilent).

**RNA Sequencing.** Total RNA was treated with the MICROBExpress Bacterial mRNA Enrichment kit (Ambion) following the manufacturer's instructions. rRNA removal was evaluated using the Agilent 2100 Bioanalyzer. mRNA-enriched RNAs were chemically fragmented to the size range of 200–250 bp using 1 $\times$  fragmentation solution (Ambion) for 5 min at 70 °C. Double-stranded cDNA was generated using the SuperScript Double-Stranded cDNA Synthesis Kit (Invitrogen). Briefly, first-strand cDNA was synthesized using SuperScript II and random hexamers, and second-strand cDNA was synthesized using *E. coli* RNaseH, ligase, and DNA polymerase I for nick translation. The Illumina Paired End Sample Prep kit was used for RNA-Seq library creation according to the manufacturer's instructions as follows: Fragmented cDNA was end-repaired, ligated to Illumina adaptors, and amplified by 10 cycles of PCR. Single or paired-end 36-bp reads were generated by sequencing using the Illumina Genome Analyzer II instrument.

**RNA-Seq Read Counts and Normalization.** RNA-Seq reads were aligned to the *E. lignolyticus* SCF1 reference genome [GenBank accession no. CP002272.1; this organism was previously called *Enterobacter cloacae* SCF1 and has been renamed *E. lignolyticus* SCF1 (26), with the old name retained in the National Center for Biotechnology Information database] using the Burrows-Wheeler Aligner (BWA) (68). Read counts were determined for each library on a per-gene basis. We normalized raw read counts by dividing by a size factor for each library, as proposed by Anders and Huber (41) and Robinson and Oshlack (69), such that the median fold change between libraries approximates 1:

$$\hat{s}_j = \text{median}_i \frac{k_{ij}}{\left( \prod_{v=1}^m k_{iv} \right)^{1/m}},$$

where  $k_{ij}$  is the raw read count for gene  $i$  in library  $j$  and  $\hat{s}_j$  is the size factor for library  $j$ . Because longer transcripts will tend to generate more RNA-Seq

reads, the normalized read counts were further divided by the length of the gene in kilobase pairs to allow comparisons across genes and comparisons with qPCR data. Raw and normalized counts for the entire dataset are included in [Dataset S1](#).

**RNA-Seq Differential Expression Analysis.** Pair-wise differential expression analysis between 375 mM [C<sub>2</sub>mim]Cl and control and between 375 mM [C<sub>2</sub>mim]Cl and 375 mM NaCl conditions at OD<sub>600</sub> = 0.6 were performed using the R package DESeq (41), available under Bioconductor ([www.bioconductor.org](http://www.bioconductor.org)). DESeq normalizes the raw counts using size factors as described above. Because estimates of variance per gene based on only two replicates are highly unreliable, DESeq uses an unbiased variance estimator that is based on a local regression against the mean expression level across the entire dataset, and then uses a negative binomial model to test for differential expression. The resulting *P* values were adjusted for multiple hypothesis testing with the procedure of Benjamini and Hochberg for controlling the false discovery rate (70). Genes with an adjusted *P* value <0.1 and a fold-change greater than 2 were assigned as differentially expressed. DESeq output tables are included in [Dataset S1](#). Fold changes for the enterobactin and ABC transporter operons were calculated by adding the RNA-Seq counts for the individual genes, without adjusting for transcript length.

**Metabolic Network Reconstruction.** The metabolic Pathway-Genome Database for SCF1 was computationally generated using Pathway Tools software version 12.5 (43) and MetaCyc version 12.5 (71), based on the genome annotation from the Joint Genome Institute's Integrated Microbial Genomics (IMG)

*niae* MGH78578, and retained the transporter families and substrate predictions for the best hits with an E-value <1 E<sup>-10</sup>. Annotations from the IMG system, RAST, MicrobesOnline, and TransportDB were combined and curated manually to remove any likely nontransporters and to assign likely substrate categories.

**RT-qPCR.** cDNA was synthesized using the SuperScript III First-Strand Synthesis System for RT-PCR (Invitrogen) according to the manufacturer's protocol, using random hexamers and a total input of 100 ng of RNA in each reaction. cDNA samples were used at 1:100 final concentration. Primers were used at 200 nM and are listed in [Table S3](#). Reactions in a 20-μL volume were run on the StepOnePlus instrument (Applied Biosystems) using PerfeCta SYBR Green SuperMix mix with ROX (Quanta Biosciences) according to the manufacturer's instructions. UbiD decarboxylase gene (Entcl\_4195) was used as a reference based on its expression stability across all conditions in the RNA-Seq dataset. Six dilutions of cDNA were used to run a standard curve for each primer, and primer efficiency (*E*) was calculated by the equation  $E = 10^{-1/m}$ , where *m* is the slope of the curve (76, 77). Ratio of expression (*R*) was quantified by the Pfaffl method (77, 78) using the equation:

$$R = \frac{(E_{\text{target}})^{\Delta C_{\text{Ttarget}}^{\text{(control-sample)}}}}{(E_{\text{reference}})^{\Delta C_{\text{Treference}}^{\text{(control-sample)}}}}$$

*R* values for each biological replicate were averaged, and the averages were log<sub>2</sub>-transformed. Error of *R* values ( $\Delta R$ ) was calculated by the following equation:

$$\Delta R = R \cdot \sqrt{\left[ \ln(E_{\text{target}}) \cdot \sqrt{(\Delta C_{\text{Ttarget}})^2 + (\Delta S_{\text{target}})^2} \right]^2 + \left[ \ln(E_{\text{reference}}) \cdot \sqrt{(\Delta C_{\text{Treference}})^2 + (\Delta S_{\text{reference}})^2} \right]^2},$$

system (72), supplemented with additional Enzyme Commission numbers from Rapid Annotation using Subsystem Technology (RAST) (73). It has undergone minimal manual curation and may contain some errors, similar to a tier 3 BioCyc Pathway-Genome Database (74). Functional annotations for the significantly differentially expressed genes are included in [Dataset S1](#).

**Transporter Substrate Category Assignments.** Putative transporters and substrate assignments were derived from a number of different annotation sources. To supplement the genome annotation from the IMG system (72), we also consulted transporter annotations generated by RAST (73) and the SCF1 genome annotation by MicrobesOnline (75), scanning for the keywords "transport," "export," "import," "symport," "antiport," "efflux," "permease," and "porin." In addition, we used BLAST to search for all SCF1 protein sequences against transporters annotated for the two closest strains in the TransportDB database (45), *Klebsiella pneumoniae* Kp342 and *K. pneumo-*

where  $\Delta S$  is the SD of  $\Delta C_T$  of three technical replicates.

**ACKNOWLEDGMENTS.** We thank Christa Pennacchio, Feng Chen, Zhong Wang, Tanja Woyke, Lynne Goodwin, and Tijana Glavina del Rio for assistance with the RNA sequencing project; Aindriia Mukhopadhyay, Mario Ouellet, Adrienne McKee, Swapnil Chhabra, and Joseph Schramm for intellectual input, experimental design, and technical advice; Anthe George and Kim Tran for providing ionic liquid reagents and technical advice; and Dylan Chivian, Jason Baumohl, Keith Keller, and Paramvir Dehal for providing Microbes Online analysis tools. Work performed at the Department of Energy Joint BioEnergy Institute (<http://www.jbei.org>), Department of Energy Joint Genome Institute, and Lawrence Berkeley National Laboratory was supported by the Office of Science of the US Department of Energy through Contract DE-AC02-05CH11231, and at Lawrence Livermore National Laboratory through Contract DE-AC52-07NA27344.

- US Department of Energy (2006) *Breaking the Biological Barriers to Cellulosic Ethanol: A Joint Research Agenda*. Report from the December 2005 Workshop, DOE/SC-0095, US Department of Energy Office of Science. Available at [www.genomicscience.energy.gov/biofuels/2005workshop/](http://www.genomicscience.energy.gov/biofuels/2005workshop/).
- Simmons BA, Loque D, Blanch HW (2008) Next-generation biomass feedstocks for biofuel production. *Genome Biol* 9:242.
- Himmel ME, et al. (2007) Biomass recalcitrance: Engineering plants and enzymes for biofuels production. *Science* 315:804–807.
- Cosgrove DJ (2005) Growth of the plant cell wall. *Nat Rev Mol Cell Biol* 6:850–861.
- Achyuthan KE, et al. (2010) Supramolecular self-assembled chaos: Polyphenolic lignin's barrier to cost-effective lignocellulosic biofuels. *Molecules* 15:8641–8688.
- da Costa Sousa L, Chundawat SP, Balan V, Dale BE (2009) 'Cradle-to-grave' assessment of existing lignocellulose pretreatment technologies. *Curr Opin Biotechnol* 20:339–347.
- Li C, et al. (2010) Comparison of dilute acid and ionic liquid pretreatment of switchgrass: Biomass recalcitrance, delignification and enzymatic saccharification. *Bioresour Technol* 101:4900–4906.
- Cheng G, et al. (2011) Transition of cellulose crystalline structure and surface morphology of biomass as a function of ionic liquid pretreatment and its relation to enzymatic hydrolysis. *Biomacromolecules* 12:933–941.
- Singh S, Simmons BA, Vogel KP (2009) Visualization of biomass solubilization and cellulose regeneration during ionic liquid pretreatment of switchgrass. *Biotechnol Bioeng* 104:68–75.
- Mora-Pale M, Meli L, Doherty TV, Linhardt RJ, Dordick JS (2011) Room temperature ionic liquids as emerging solvents for the pretreatment of lignocellulosic biomass. *Biotechnol Bioeng* 108:1229–1245.
- Pham TP, Cho CW, Yun YS (2010) Environmental fate and toxicity of ionic liquids: A review. *Water Res* 44:352–372.
- Quijano G, Couvert A, Amrane A (2010) Ionic liquids: Applications and future trends in bioreactor technology. *Bioresour Technol* 101:8923–8930.
- Romero A, Santos A, Tojo J, Rodriguez A (2008) Toxicity and biodegradability of imidazolium ionic liquids. *J Hazard Mater* 151:268–273.
- Xu Q, Singh A, Himmel ME (2009) Perspectives and new directions for the production of bioethanol using consolidated bioprocessing of lignocellulose. *Curr Opin Biotechnol* 20:364–371.
- Elkins JG, Raman B, Keller M (2010) Engineered microbial systems for enhanced conversion of lignocellulosic biomass. *Curr Opin Biotechnol* 21:657–662.
- Margeot A, Hahn-Hagerdal B, Edlund M, Slade R, Monot F (2009) New improvements for lignocellulosic ethanol. *Curr Opin Biotechnol* 20:372–380.
- Connor MR, Liao JC (2009) Microbial production of advanced transportation fuels in non-natural hosts. *Curr Opin Biotechnol* 20:307–315.
- Nicolaou SA, Gaida SM, Papoutsakis ET (2010) A comparative view of metabolite and substrate stress and tolerance in microbial bioprocessing: From biofuels and chemicals, to biocatalysis and bioremediation. *Metab Eng* 12:307–331.
- Docherty KM, Kulpa CF (2005) Toxicity and antimicrobial activity of imidazolium and pyridinium ionic liquids. *Green Chem* 7:185–189.
- Ganske F, Bornscheuer UT (2006) Growth of *Escherichia coli*, *Pichia pastoris* and *Bacillus cereus* in the presence of the ionic liquids [BMIM][BF<sub>4</sub>] and [BMIM][PF<sub>6</sub>] and Organic Solvents. *Biotechnol Lett* 28:465–469.
- Lee SM, Chang WJ, Choi AR, Koo YM (2005) Influence of ionic liquids on the growth of *Escherichia coli*. *Korean J Chem Eng* 22:687–690.
- Matsumoto M, Mochiduki K, Kondo K (2004) Toxicity of ionic liquids and organic solvents to lactic acid-producing bacteria. *J Biosci Bioeng* 98:344–347.

23. DeAngelis KM, et al. (2011) Characterization of trapped lignin-degrading microbes in tropical forest soil. *PLoS ONE* 6:e19306.
24. Allgaier M, et al. (2010) Targeted discovery of glycoside hydrolases from a switchgrass-adapted compost community. *PLoS ONE* 5:e8812.
25. Reddy AP, et al. (2011) Bioenergy feedstock-specific enrichment of microbial populations during high-solids thermophilic deconstruction. *Biotechnol Bioeng* 108:2088–2098.
26. DeAngelis KM, et al. (2011) Complete genome sequence of “Enterobacter lignolyticus” SCF1. *Stand Genomic Sci* 5:69–85.
27. Zavrel M, Bross D, Funke M, Büchs J, Spiess AC (2009) High-throughput screening for ionic liquids dissolving (ligno-)cellulose. *Bioresour Technol* 100:2580–2587.
28. Bochner BR (2003) New technologies to assess genotype-phenotype relationships. *Nat Rev Genet* 4:309–314.
29. Bochner BR, Savageau MA (1977) Generalized indicator plate for genetic, metabolic, and taxonomic studies with microorganisms. *Appl Environ Microbiol* 33:434–444.
30. Borglin S, et al. (2012) Application of phenotypic microarrays to environmental microbiology. *Curr Opin Biotechnol* 23:41–48.
31. Borglin S, Joyner D, Jacobsen J, Mukhopadhyay A, Hazen TC (2009) Overcoming the anaerobic hurdle in phenotypic microarrays: Generation and visualization of growth curve data for *Desulfovibrio vulgaris* Hildenborough. *J Microbiol Methods* 76:159–168.
32. Zwietering MH, Jongenburger I, Rombouts FM, van't Riet K (1990) Modeling of the bacterial growth curve. *Appl Environ Microbiol* 56:1875–1881.
33. Baba T, et al. (2006) Construction of *Escherichia coli* K-12 in-frame, single-gene knockout mutants: The Keio collection. *Mol Syst Biol* 2:1–11.
34. Docherty KM, Dixon JK, Kulpa CF, Jr. (2007) Biodegradability of imidazolium and pyridinium ionic liquids by an activated sludge microbial community. *Biodegradation* 18:481–493.
35. Empadinhas N, da Costa MS (2008) Osmoadaptation mechanisms in prokaryotes: Distribution of compatible solutes. *Int Microbiol* 11:151–161.
36. Zhang YM, Rock CO (2008) Membrane lipid homeostasis in bacteria. *Nat Rev Microbiol* 6:222–233.
37. Cronan JE, Jr. (2002) Phospholipid modifications in bacteria. *Curr Opin Microbiol* 5:202–205.
38. Ramos JL, et al. (2002) Mechanisms of solvent tolerance in gram-negative bacteria. *Annu Rev Microbiol* 56:743–768.
39. Wang Z, Gerstein M, Snyder M (2009) RNA-Seq: A revolutionary tool for transcriptomics. *Nat Rev Genet* 10:57–63.
40. van Vliet AH (2010) Next generation sequencing of microbial transcriptomes: Challenges and opportunities. *FEMS Microbiol Lett* 302:1–7.
41. Anders S, Huber W (2010) Differential expression analysis for sequence count data. *Genome Biol* 11:R106.
42. Weber H, Polen T, Heuveling J, Wendisch VF, Hengge R (2005) Genome-wide analysis of the general stress response network in *Escherichia coli*: SigmaS-dependent genes, promoters, and sigma factor selectivity. *J Bacteriol* 187:1591–1603.
43. Karp PD, Paley S, Romero P (2002) The Pathway Tools software. *Bioinformatics* 18(Suppl 1):S225–S232.
44. Zafarani-Moattar MT, Sarmad S (2011) Osmotic and activity coefficient of 1-ethyl-3-methylimidazolium chloride in aqueous solutions of tri-potassium phosphate, potassium carbonate, and potassium chloride at T = 298.15 K. *Calphad* 35:331–341.
45. Ren Q, Chen K, Paulsen IT (2007) TransportDB: A comprehensive database resource for cytoplasmic membrane transport systems and outer membrane channels. *Nucleic Acids Res* 35(Database issue):D274–D279.
46. Fernandes P, Ferreira BS, Cabral JM (2003) Solvent tolerance in bacteria: Role of efflux pumps and cross-resistance with antibiotics. *Int J Antimicrob Agents* 22:211–216.
47. Delcour AH (2009) Outer membrane permeability and antibiotic resistance. *Biochim Biophys Acta* 1794:808–816.
48. Dunlop MJ, et al. (2011) Engineering microbial biofuel tolerance and export using efflux pumps. *Mol Syst Biol* 7:487.
49. Davin-Regli A, et al. (2008) Membrane permeability and regulation of drug “influx and efflux” in enterobacterial pathogens. *Curr Drug Targets* 9:750–759.
50. Chang YY, Cronan JE, Jr. (1999) Membrane cyclopropane fatty acid content is a major factor in acid resistance of *Escherichia coli*. *Mol Microbiol* 33:249–259.
51. Shabala L, Ross T (2008) Cyclopropane fatty acids improve *Escherichia coli* survival in acidified minimal media by reducing membrane permeability to H<sup>+</sup> and enhanced ability to extrude H<sup>+</sup>. *Res Microbiol* 159:458–461.
52. Zhao Y, et al. (2003) Expression of a cloned cyclopropane fatty acid synthase gene reduces solvent formation in *Clostridium acetobutylicum* ATCC 824. *Appl Environ Microbiol* 69:2831–2841.
53. Machado MC, López CS, Heras H, Rivas EA (2004) Osmotic response in *Lactobacillus casei* ATCC 393: Biochemical and biophysical characteristics of membrane. *Arch Biochem Biophys* 422:61–70.
54. Broadbent JR, Larsen RL, Deibel V, Steele JL (2010) Physiological and transcriptional response of *Lactobacillus casei* ATCC 334 to acid stress. *J Bacteriol* 192:2445–2458.
55. Escobar L, Pérez-Martín J, de Lorenzo V (1999) Opening the iron box: Transcriptional metalloregulation by the Fur protein. *J Bacteriol* 181:6223–6229.
56. Kunin CM, Tong HH, Maher WE (1993) Naturally-occurring, osmo-remedial variants of *Escherichia coli*. *J Med Microbiol* 38:216–221.
57. Tschuch A, Pfennig N (1984) Growth-yield increase linked to caffeine reduction in *Acetobacterium-woodii*. *Arch Microbiol* 137:163–167.
58. Widdel F, Kohring GV, Mayer F (1983) Studies on dissimilatory sulfate-reducing bacteria that decompose fatty-acids. 3. Characterization of the filamentous gliding *Desulfonema-Limicola* Gen-Nov Sp-Nov, and *Desulfonema-Magnum* Sp-Nov. *Arch Microbiol* 134:286–294.
59. Janssen PH, Schuhmann A, Mörschel E, Rainey FA (1997) Novel anaerobic ultramicrobacteria belonging to the *Verrucomicrobiales* lineage of bacterial descent isolated by dilution culture from anoxic rice paddy soil. *Appl Environ Microbiol* 63:1382–1388.
60. White DC, Ringelberg DB (1998) *Signature Lipid Biomarker Analysis. Techniques in Microbial Ecology* (Oxford Univ Press, New York), pp 255–272.
61. Guckert JB, Antworth CP, Nichols PD, White DC (1985) Phospholipid, ester-linked fatty-acid profiles as reproducible assays for changes in prokaryotic community structure of estuarine sediments. *FEMS Microbiol Ecol* 31:147–158.
62. Pfiffner SM, et al. (2006) Deep subsurface microbial biomass and community structure in Witwatersrand Basin mines. *Geomicrobiol J* 23:431–442.
63. Griffiths BS, Ritz K, Ebbelwhite N, Dobson G (1999) Soil microbial community structure: Effects of substrate loading rates. *Soil Biol Biochem* 31:145–153.
64. Salomonova S, et al. (2003) Determination of phospholipid fatty acids in sediments. *Chimica* 42:39–49.
65. Steger K, Jarvis A, Smårs S, Sundh I (2003) Comparison of signature lipid methods to determine microbial community structure in compost. *J Microbiol Methods* 55:371–382.
66. Moore-Kucera J, Dick RP (2008) PLFA profiling of microbial community structure and seasonal shifts in soils of a Douglas-fir chronosequence. *Microb Ecol* 55:500–511.
67. Cusack DF, Silver WL, Torn MS, Burton SD, Firestone MK (2011) Changes in microbial community characteristics and soil organic matter with nitrogen additions in two tropical forests. *Ecology* 92:621–632.
68. Li H, Durbin R (2009) Fast and accurate short read alignment with Burrows-Wheeler transform. *Bioinformatics* 25:1754–1760.
69. Robinson MD, Oshlack A (2010) A scaling normalization method for differential expression analysis of RNA-seq data. *Genome Biol* 11:R25.
70. Benjamini Y, Hochberg Y (1995) Controlling the false discovery rate: A practical and powerful approach to multiple testing. *J R Stat Soc Series B Stat Methodol* 57:289–300.
71. Caspi R, et al. (2008) The MetaCyc Database of metabolic pathways and enzymes and the BioCyc collection of Pathway/Genome Databases. *Nucleic Acids Res* 36(Database issue):D623–D631.
72. Markowitz VM, et al. (2010) The integrated microbial genomes system: An expanding comparative analysis resource. *Nucleic Acids Res* 38(Database issue):D382–D390.
73. Aziz RK, et al. (2008) The RAST Server: Rapid annotations using subsystems technology. *BMC Genomics* 9:75.
74. Karp PD, et al. (2005) Expansion of the BioCyc collection of pathway/genome databases to 160 genomes. *Nucleic Acids Res* 33:6083–6089.
75. Dehal PS, et al. (2010) MicrobesOnline: An integrated portal for comparative and functional genomics. *Nucleic Acids Res* 38(Database issue):D396–D400.
76. Ramakers C, Ruijter JM, Deprez RH, Moorman AF (2003) Assumption-free analysis of quantitative real-time polymerase chain reaction (PCR) data. *Neurosci Lett* 339:62–66.
77. Pfaffl MW (2001) A new mathematical model for relative quantification in real-time RT-PCR. *Nucleic Acids Res* 29:e45.
78. Ouellet M, Adams PD, Keasling JD, Mukhopadhyay A (2009) A rapid and inexpensive labeling method for microarray gene expression analysis. *BMC Biotechnol* 9:97.